F-18 Stilbenes as PET Imaging Agents for Detecting β-Amyloid Plaques in the Brain

Wei Zhang,[†] Shunichi Oya,[†] Mei-Ping Kung,[†] Catherine Hou,[†] Donna L. Maier,[‡] and Hank F. Kung*[,†,§]

Departments of Radiology and Pharmacology, University of Pennsylvania, Philadelphia, Pennsylvania 19104, and Department of Neuroscience, AstraZeneca, Wilmington, Delaware 19850

Received February 21, 2005

Imaging agents targeting β-amyloid (Aβ) may be useful for diagnosis and treatment of patients with Alzheimer's disease (AD). Compounds **3e** and **4e** are fluorinated stilbene derivatives displaying high binding affinities for Aβ plaques in AD brain homogenates ($K_i = 15 \pm 6$ and 5.0 ± 1.2 nM, respectively). In vivo biodistributions of [^{18}F]**3e** and [^{18}F]**4e** in normal mice exhibited excellent brain penetrations (5.55 and 9.75% dose/g at 2 min), and rapid brain washouts were observed, especially for [^{18}F]**4e** (0.72% dose/g at 60 min). They also showed in vivo plaque labeling in APP/PS1 or Tg2576 transgenic mice, animal models for AD. Autoradiography of postmortem AD brain sections and AD homogenate binding studies confirmed the selective and specific binding properties to Aβ plaques. In conclusion, the preliminary results strongly suggest that these fluorinated stilbene derivatives, [^{18}F]**3e** and [^{18}F]**4e**, are suitable candidates as Aβ plaque imaging agents for studying patients with AD.

Introduction

Alzheimer's disease (AD) is a brain disorder associated with progressive memory loss and decrease of cognitive function. Currently, a definitive diagnosis of AD can only be established by demonstrating the presence of abundant senile plaques and neurofibrillary tangles in the postmortem brain.[1,2] The senile plaques are extracellular deposits of amyloid fibrils of β-amyloid (Aβ), and their presence is strongly associated with pathogenesis of the disease. Thus, specific in vivo imaging agents targeting Aβ plaques may serve as suitable markers for monitoring the amyloid burden following the disease progression and further provide supporting evidence for therapeutic intervention.[3] Currently, many efforts focusing on development of therapeutic approach targeting Aβ plaques or reversing the effects of the plaque-deposition have been reported.[4,5]

Development of imaging agents for direct mapping of Aβ aggregates in the living brain is an active research area in recent years. Several research groups have reported biomarkers for imaging Aβ plaques in the brain.[6−10] The Aβ-plaque-specific imaging agents can be labeled with short-lived isotopes suitable for in vivo imaging studies.[10] Two isotopes,^{99m}Tc ($T_{1/2}$, 6 h, 140 keV) and ^{123}I ($T_{1/2}$, 13 h, 159 keV), are commonly used for single photon emission computed tomography (SPECT); while ^{11}C ($T_{1/2}$, 20 min, 511 keV) and ^{18}F ($T_{1/2}$, 110 min, 511 keV) are often used for positron emission tomography (PET). It is generally accepted that SPECT is more convenient and cost-effective, but PET gives a better imaging resolution. Recently, successful preliminary reports using a ^{11}C-labeled benzothiazole derivative, [^{11}C]PIB,[6,11,12] and a ^{18}F-labeled probe, [^{18}F]FDDNP,[9,13,14] for plaque and tangle visualization in living AD patients have demonstrated the potential utility of in vivo imaging (Figure 1). Similarly, our group has also prepared a ^{11}C-labeled PET ligand, [^{11}C]SB-13 (4-*N*-methylamino-4′-hydroxystilbene), a stilbene derivative,[7,15] and a ^{123}I-labeled SPECT ligand, IMPY (6-iodo-2-(4′-*N*,*N*-dimethylamino)phenylimidazo[1,2-*a*]-pyridine).[16−18] Both tracers showed selective and high binding affinities to Aβ plaques.[19] As expected, [^{11}C]SB-13 displayed a high accumulation in the frontal cortex (presumably an area containing a high density of Aβ plaques) in mild to moderate AD patients, but not in age-matched control subjects;[7] while the SPECT ligand, [^{123}I[IMPY, is currently under active clinical evaluation. Other structurally similar compounds have been recently reported for targeting Aβ plaques in the brain.[20−22]

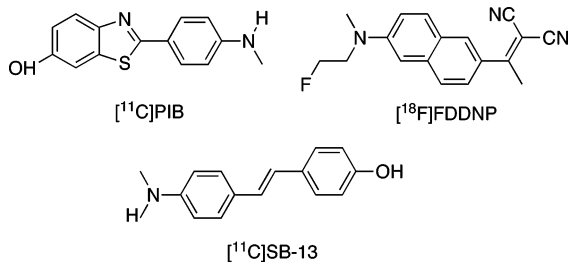

Figure 1. Structures of PET imaging agents proven to target amyloid plaques in AD patients.

Initially, we reported an iodinated derivative of stilbene, 3-iodo-4′-diaminostilbene, targeting amyloid plaques for SPECT imaging.[23] However, the unfavorable in vivo kinetic properties make it unattractive for further development as a useful in vivo SPECT tracer for amyloid plaques in the brain. We have subsequently identified another stilbene derivative, SB-13, labeled with C-11 as a potential PET tracer for plaque imaging.[15] It was clinically demonstrated that [^{11}C]SB-13 can detect senile plaques present in AD patients.[7] However,

* Hank F. Kung, Ph.D., Department of Radiology, University of Pennsylvania, 3700 Market St., Rm. 305, Philadelphia, PA 19104. Tel: (215)662-3096, Fax: (215)349-5035; e-mail: kunghf@sunmac.spect.upenn.edu.

[†] Department of Radiology, University of Pennsylvania.

[‡] AstraZeneca.

[§] Department of Pharmacology, University of Pennsylvania.

10.1021/jm050166g CCC: $30.25
Published on Web 08/23/2005

Scheme 1[a]

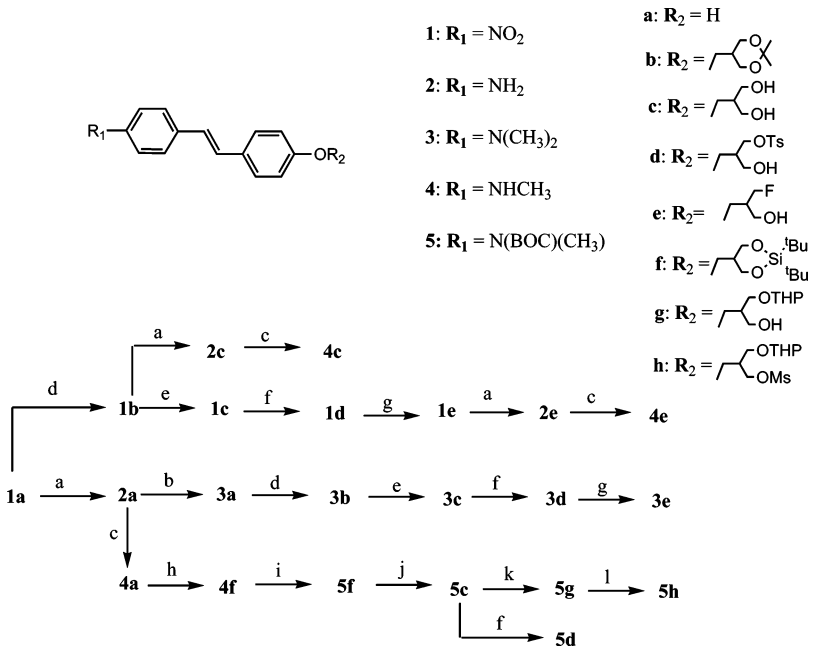

[a] (a) $SnCl_2$, HCl(c), EtOH; (b) (CHO)n, $NaBH_3CN$, AcOH, rt; (c) (1) NaOMe, MeOH, $(CHO)_n$; (2) $NaBH_4$; (d) **8m**, K_2CO_3, DMF, 100 °C; (e) HCl, CH_3COCH_3, rt; (f) TsCl, Py, 0 °C; (g) TBAF, THF, reflux; (h) **8n**, K_2CO_3, DMF, 100 °C; (i) $(BOC)_2O$, THF, reflux; (j) TBAF (1 M), THF, rt; (k) DHP, PPTS, DCM, rt; (l) MsCl, Et_3N, DCM, rt.

the short half-life (20 min) of C-11 may limit the usefulness of [^{11}C]SB-13 or [^{11}C]PIB for a widespread clinical application. One major focus of our effort is in development of ^{18}F-labeled plaque-specific imaging agents, because the longer half-life of F-18 and stability in solution allow the use of the radioligand over a long period of time. While this work was in progress a series of ^{18}F-labeled styrylbenzoxazole compounds, such as 2-(4-methylaminostyryl)-6-(2-[^{18}F]fluoroethoxy) benzoxazole, were reported to show promise as potential PET imaging agents targeting amyloid plaques in the brain.[8]

Reported herein are the synthesis and in vitro and in vivo evaluations of a novel series of two ^{18}F-labeled stilbene derivatives as prospective PET radiotracers for imaging amyloid plaques in the brain.

Results and Discussion:

Chemistry. Syntheses of compounds **3e**, **4e** and radiolabelings of precursors **3d**, **5h** to prepare [^{18}F]**3e** and [^{18}F]**4e** are shown in Scheme 1 and Scheme 4. To prepare compound **3a** the nitro group of 4-nitro-4′-hydroxystilbene, **1a**, was reduced with $SnCl_2$/HCl(c) in ethanol to give the corresponding amine **2a**. Following a treatment with $(CHO)_n$ and $NaBH_3CN$, the dimethylamino compound **3a** was obtained. Compound **3b** was obtained by reacting the hydroxylstilbene **3a** with bromide **8m**,[24] which was separately prepared as shown in Scheme 2, and potassium carbonate in anhydrous DMF. Compound **3c** was obtained by treatment of **3b** with 1 N HCl in acetone to remove the protected group. Reacting diol **3c** with 1.5 equiv of tosyl chloride in pyridine gave a mixture; however, monotosylate **3d** could be isolated from the mixture by silica gel chromatography with 5% methanol in dichloromethane as the eluent. The tosylate group of **3d** was converted to fluoride **3e** by refluxing with anhydrous TBAF in THF.[25] The tosyl compound **3d** was also used as the starting material to obtain radiolabeled compound, [^{18}F]**3e**. Nitro

Scheme 2[a]

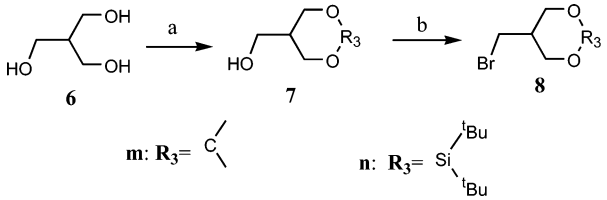

[a] (a) **7m**: $(CH_3O)_2C(CH_3)_2$, TsOH, reflux; **7n**: HOBT, Si(*t*-Bu)$_2$Cl$_2$, Et3N, DCM, reflux; (b) CBr_4, PPh_3, Py, DCM, rt.

compound **1e** was similarly synthesized by a coupling reaction of **1a** with **8m**[24] followed by tosylation and fluorination. The synthesis of compound **4e** was accomplished by reduction of the nitro group of **1e** with $SnCl_2$/EtOH followed by a monomethylation of the amino group with $(CHO)_n$, $NaOCH_3$, and $NaBH_4$. The nitro group of the acetal-protected intermediate **1b** was reduced to amine **2c** and then monomethylated to give compound **4c**. Similarly, **2a** was first monomethylated to give the compound **4a**, after which **4a** was coupled with **8n** to give **5f**. The di-*tert*-butylsilyl group of **5f** was removed with 1 N TBAF in THF at room temperature to give diol **5c.** The obtained **5c** could be either monotosylated to give **5d** or monoprotected by THP[26] to give **5g**. From **5g**, the desired mesylated precusor **5h** for radiolabeling can thus be obtained.

A related *p*-bromobenzyl compound **3j** was also synthesized as shown in Scheme 3. The substituted malonate **9**[27] was reduced to diol **10** with DIBALH and then reacted with 1 equiv of TBSCl to give **11**. The unprotected OH was then converted into bromide **12** with CBr_4/PPh_3. Compound **12** was reacted with **3a** to give **3i** which was treated with TBAF to remove TBS group to yield **3j**.

Several starting materials were evaluated in a radiofluoride displacement reaction. To obtain dimethylamino derivative [^{18}F]**3e**, the tosylated precursor **3d** was

Scheme 3[a]

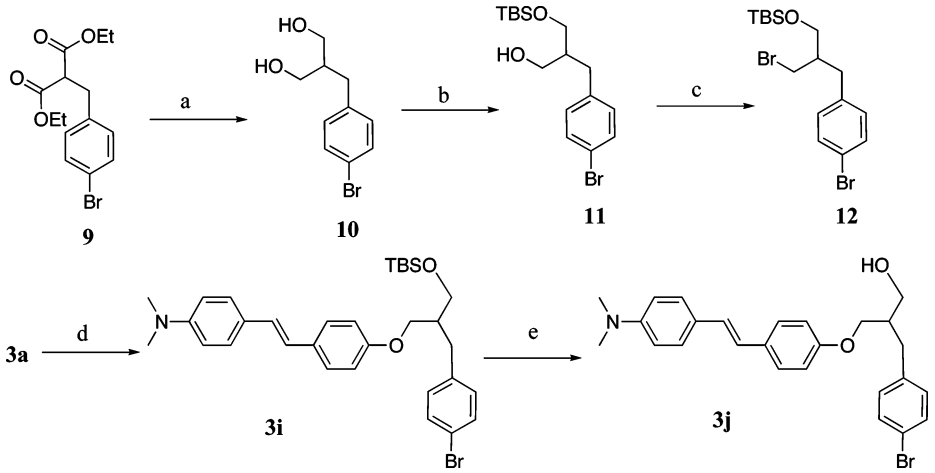

[a] (a) DIBALH, THF, 0 °C; (b) TBSCl, Et_3N, DCM, rt; (c) CBr_4, PPh_3, DCM, rt; (d) K_2CO_3, **12**, DMF, 100 °C; (e) TBAF(1 M), THF, rt.

Scheme 4[a]

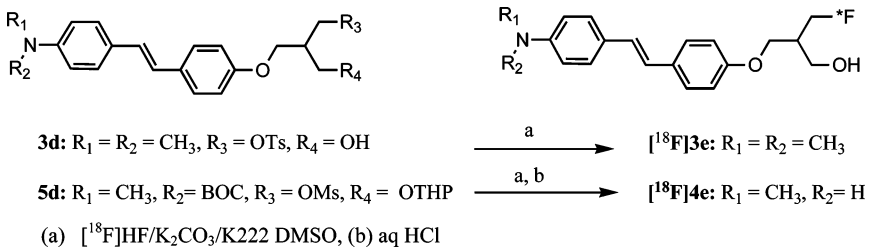

[a] (a) [^{18}F]HF/K_2CO_3/K222 DMSO, (b) aq HCl.

mixed with [^{18}F]fluoride/potassium carbonate and Kryptofix 222 in DMSO and heated at 120 °C for 4 min (Scheme 4). Crude product was purified by HPLC to attain >99% of the radiochemical purity with 10% radiochemical yield (decay corrected). The procedure took 90 min, and specific activity was estimated to be 70 Ci/mmol at the end of synthesis. To obtain the *N*-monomethyl derivative [^{18}F]**4e**, tosylate **5d** was first prepared as the precursor for radiolabeling. However, the purification of [^{18}F]**4e** was tedious and time-consuming resulting in a low yield. The situation was greatly improved when using **5h** as the precursor for labeling, of which mesylate was used instead of tosylate, and the free OH was protected with THP. An advantage of using mesylate **5h** as the radiolabeling precursor is that reaction proceeded more cleanly. As a result, the amount and the number of unknown side-products were significantly reduced. Specific activity estimated by comparing UV peak intensity of labeled compound with reference nonradioactive compound of known concentration improved at least 10 times at the end of synthesis comparing with that obtained from tosylated precursor **5d**. A similar procedure was carried out to obtain [^{18}F]-**4e** from the mesylated precursor **5h**. After the initial reaction in DMSO, the mixture was treated with aqueous HCl to remove BOC and THP groups. Radiochemical purity was >99% after HPLC purification and the radiochemical yield was 20% (decay corrected). The total syntheses took 110 min and specific activity was estimated to be 900−1000 Ci/mmol at the end of synthesis.

Biological Studies. Binding affinities of the new series of stilbene derivatives were examined in a binding assay using AD brain homogenates and [^{125}I]IMPY as the radioligand.[19] Compound **4a** (SB-13), as shown previously, displayed a high binding affinity.[19] With an additional methyl group attached to the nitrogen atom (dimethylamino vs monomethylamino in **3a** vs **4a**), a similar high binding affinity was observed (1.1 nM and 1.2 nM for **3a** and **4a**, respectively) (Table 1). Further modifications of **3a** result in epoxy and diol derivatives **3b** and **3c**, but they showed lower binding affinities (K_i = 59 and 38 nM, respectively). A relatively high binding affinity (K_i = 15 nM) was obtained with **3e** (a fluorinated derivative).

Table 1. Inhibition Constants (K_i, nM) of Compounds on I-125-IMPY Binding to Amyloid Plaques in AD Brain Homogenates

compound	$K_i \pm$ SEM (nM)[a]	compound	$K_i \pm$ SEM (nM)[a]
2a	95 ± 8.0	**3e**	15 ± 6
2e	15 ± 4.0	**3j**	80 ± 20
3a	1.1 ± 0.2	**4a** (SB-13)	1.2 ± 0.2*
3b	59 ± 10	**4c**	32.5 ± 5.0
3c	38 ± 5	**4e**	5.0 ± 1.2
3d	150 ± 30	PIB	2.8 ± 0.5

[a] Each value was determined three times with duplicate for each measurement. [b] The value was reported previously.[19]

Since the binding affinity of **3e** appeared promising, the corresponding tosylated derivative **3d** was prepared as a starting material for radiolabeling with ^{18}F. Under the chosen HPLC conditions (Hamilton PRP-1 column, CH_3CN/dimethyl glutarate buffer (5 mM, pH 7) = 9/1), the tosylated and the diol derivatives can be clearly separated from the desired ^{18}F-labeled stilbene [^{18}F]**3e**. This HPLC system has been successfully applied to remove the potential pseudo-carrier, the hydroxyl compound **3c**. Similarly, the monomethylamino compounds displayed the same trend with a high affinity for the fluorinated derivative **4e** (K_i = 5 nM) and a lower

Table 2. Biodistribution in ICR Mice after an iv Injection of [^{18}F]Tracers in 0.1% BSA (%dose/g, avg of three mice ± SD)

organ	2 min	30 min	1 h	2 h
	[^{18}F]**3e** (Partition Coefficient = 1375)			
blood	1.79 ± 0.25	1.65 ± 0.15	1.51 ± 0.20	1.18 ± 0.08
heart	10.43 ± 0.96	2.76 ± 0.26	1.45 ± 0.17	0.91 ± 0.04
muscle	0.84 ± 0.30	1.53 ± 0.30	1.22 ± 0.20	0.66 ± 0.13
lung	93.40 ± 16.91	12.93 ± 4.75	5.00 ± 0.84	3.74 ± 0.35
kidney	13.32 ± 1.41	4.64 ± 0.26	2.97 ± 0.29	2.19 ± 0.26
spleen	4.43 ± 0.26	2.45 ± 0.22	1.24 ± 0.11	0.99 ± 0.14
liver	14.13 ± 0.73	14.65 ± 1.73	13.46 ± 2.62	9.51 ± 1.04
skin	0.67 ± 0.02	1.69 ± 0.38	1.65 ± 0.15	1.00 ± 0.07
brain	5.55 ± 0.64	5.21 ± 0.66	2.97 ± 0.43	1.37 ± 0.14
bone	1.57 ± 0.12	2.06 ± 0.35	6.50 ± 2.92	8.63 ± 1.78
	[^{18}F]**4e** (Partition Coefficient = 889)			
blood	2.60 ± 0.23	2.47 ± 0.25	1.82 ± 0.30	0.78 ± 0.02
heart	7.49 ± 0.95	2.06 ± 0.24	1.54 ± 0.12	0.65 ± 0.02
muscle	0.74 ± 0.11	1.31 ± 0.45	0.85 ± 0.41	0.41 ± 0.04
lung	26.13 ± 1.91	8.90 ± 1.39	7.51 ± 1.01	4.15 ± 0.61
kidney	11.70 ± 1.49	4.13 ± 0.35	3.06 ± 0.17	1.50 ± 0.08
spleen	5.01 ± 1.64	2.41 ± 0.57	1.37 ± 1.08	1.22 ± 0.34
liver	20.61 ± 2.00	19.60 ± 1.40	14.58 ± 1.35	8.14 ± 2.33
skin	0.92 ± 0.23	1.49 ± 0.25	1.22 ± 0.21	0.57 ± 0.08
brain	9.75 ± 1.38	1.70 ± 0.41	0.72 ± 0.13	0.31 ± 0.04
bone	1.53 ± 0.32	2.13 ± 0.19	5.30 ± 1.94	7.76 ± 0.29

affinity for the diol derivative **4c** (K_i = 32.5 nM). In addition, other derivatives such as *p*-bromobenzyl-substituted **3j** showed a lower binding affinity (K_i = 80 nM). Interestingly, the free amino derivative **2e**, under a similar binding assay condition, showed a K_i value of 15 ± 4.0 nM which was comparable to the dimethylamino (**3e**) and monomethylamino (**4e**) derivatives (competing with [^{125}I]IMPY binding) (Table 1). This result is different from the original stilbene compounds showing a much lower binding affinity for the free amino compound (K_i = 1.1, 1.2, and 95 nM for **3a**, **4a** (SB-13), and **2a**, respectively). Surprisingly, despite the fact that **2e** showed reasonably good in vitro binding affinity (a relatively low K_i value), [^{18}F]**2e** exhibited no specific binding signal for amyloid plaques (using either AD brain section labeling or AD homogenate binding) (data not shown). Therefore, we have abandoned this free amino compound and focused only on [^{18}F]**3e** and [^{18}F]-**4e** as likely candidates. As expected, both [^{18}F]**3e** and [^{18}F]**4e** clearly label plaques by in vitro autoradiography using postmortem AD brain sections showing a high plaque labeling and a low background (see Figure 2). The same results were obtained using brain sections of double transgenic (APP/PS1) mice (data not shown).

Previously, using an in vitro binding assay we have reported saturable and high binding affinities in postmortem brain homogenates of AD patients for two potential tracers, [^{3}H]SB-13 (a *N*-methylamino derivative) and [^{125}I]IMPY (a *N,N*-dimethylamino derivative).[19] Interestingly, [^{18}F]**3e** contains a *N,N*-dimethylamino group, but it did not display any specific Aβ plaque binding signals in the brain homogenates binding assay (data not shown). However, using a mono-*N*-methylated derivative, [^{18}F]**4e**, in the same binding assay, a distinct binding signal was observed in the gray matter homogenates of AD patients. In the white matter of AD patients, where Aβ plaque deposits were low to nonexistent, the binding signal was significantly lower (6−8 times lower) (Figure 4), whereas in assays using brain homogenates from control subjects, the binding signals in both gray and white matters were low, suggesting that the binding was highly selective to the presence of Aβ plaque deposits. The specific binding observed for [^{18}F]**4e** in AD brain homogenates was saturable, and the binding capacity (B_{max}) was in the range of 10−20 pmol/mg tissue (data not shown). Detailed in vitro binding characterization of [^{18}F]**4e** will be published elsewhere as a separate paper.

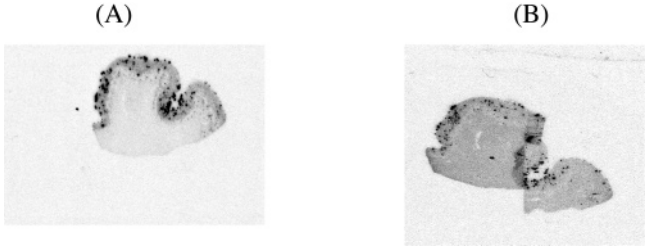

Figure 2. In vitro autoradiography of brain sections from AD patients labeled with [^{18}F]**3e** (A) and [^{18}F]**4e** (B). The Aβ plaques were clearly labeled with both ^{18}F tracers with low background labeling.

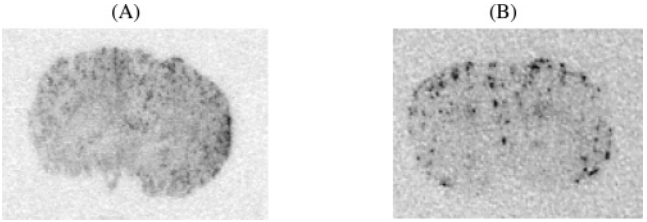

Figure 3. In vivo plaque labeling visualized by ex vivo autoradiogram: (A) [^{18}F]**3e** in a APP/PS1 mouse brain; (B) [^{18}F]-**4e** in a Tg2576 mouse. The animal was injected via tail vein with 270 μCi [^{18}F]**3e** or 260 μCi [^{18}F]**4e** and sacrificed 2 h (for [^{18}F]**3e**) or 1 h (for [^{18}F]**4e**) after tracer injection.

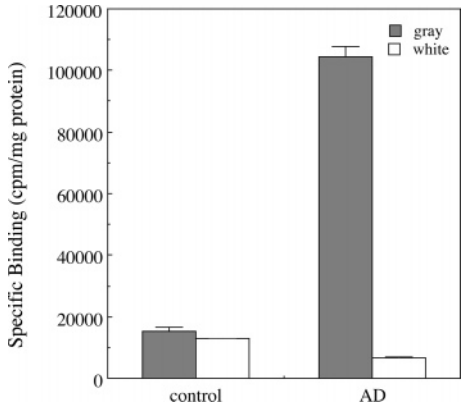

Figure 4. [^{18}F]**4e** showed binding to AD and control tissue homogenates prepared from dissected gray and white matter of cortical regions. High specific binding was detected mainly in gray matter with relatively low binding in white matter homogenates. In contrast, homogenates from the control showed significantly lower specific binding of [^{18}F]**4e**.

After an iv injection, both [^{18}F]**3e** and [^{18}F]**4e** displayed good initial brain uptakes in normal mice (5.55% and 9.75% ID/g at 2 min postinjection for [^{18}F]**3e** and [^{18}F]**4e**, respectively). The rate of washout of [^{18}F]**3e** from the brain was slower as compared to that of [^{18}F]-**4e** (1.37% and 0.31%ID/g at 120 min postinjection for [^{18}F]**3e** and [^{18}F]**4e**, respectively). A relatively higher lipophilicity was observed for [^{18}F]**3e** (partition coefficient = 1375 and 889 for [^{18}F]**3e** and [^{18}F]**4e**, respectively). This disparity may account for the longer brain retention observed for [^{18}F]**3e**. Initial blood levels were relatively low for both tracers (1.79% and 2.60% ID/g for [^{18}F]**3e** and [^{18}F]**4e**, respectively), and there was a

significant reduction at 2 h postinjection (1.18 and 0.78%ID/g). In vivo defluorination was likely for both tracers, because the bone uptake showed increasing uptake reaching 7−8%ID/g at 2 h postinjection.

To examine the in vivo labeling of Aβ plaques in a living brain, we have tested both candidates using mouse models, APP/PS1[8,28] or Tg2576 transgenic mice,[29] which are specifically engineered to over produce the Aβ plaques in the brain. When subjected to in vivo labeling of Aβ plaques (after an *iv* injection) in these models, distinctive Aβ plaque labeling can be observed for both [^{18}F]**3e** and [^{18}F]**4e** (Figure 3A and 3B). The specific in vivo targeting for Aβ plaques, especially for [^{18}F]**4e**, demonstrates the feasibility of using it as an in vivo PET imaging agent for detecting senile plaques. Both of these transgenic mouse models have been successfully used in studying relationships between deposit of Aβ plaques and AD.[30,31] For the purpose of this in vivo Aβ plaque labeling study by a ^{18}F tracer in a transgenic mouse model we did not make a distinction between using either one of these models. Recently, the presence of soluble oligomer of amyloid-β peptides, prior to their aggregation to fribrillary forms, has attracted attention as the primary underlying feature leading to neuronal toxicity and symptoms of AD.[32−34] The PET imaging agents reported in this paper will not be able to detect the soluble form of amyloid-β peptides; however, the presence of the oligomers is likely a prelude leading to the formation of Aβ aggregates in the brain. Therefore, from a diagnostic perspective, imaging agents targeting Aβ plaques in the brain will still be very useful for the diagnosis of AD. Efforts in developing novel ligands for binding the soluble Aβ oligomers will be an interesting and highly important research topic.

Conclusion

A new series of novel stilbene derivatives displaying high binding affinities to Aβ plaques was successfully prepared as potential PET imaging agents for AD. Both 4-dimethylamino and 4-monomethylamino stilbenes ([^{18}F]**3e** and [^{18}F]**4e)** entered the brain of normal mice readily and quickly. [^{18}F]**4e** showed a fast washout with a low normal brain retention. Specific plaque labeling was demonstrated by in vitro and ex vivo autoradiography of brain sections. Favorable pharmacokinetic properties and specific plaque labeling properties of these ^{18}F-labeled stilbene derivatives, especially [^{18}F]-**4e**, warrant further investigation.

Experimental Section

All reagents used in syntheses were commercial products and were used without further purification unless otherwise indicated. ^{1}H NMR spectra were obtained on a Bruker DPX spectrometer (200 MHz) in $CDCl_3$ unless otherwise indicated. Chemical shifts are reported as δ values (parts per million) relative to internal TMS. Coupling constants are reported in Hertz. The multiplicity is defined by s (singlet), d (doublet), t (triplet), br (broad), m (multiplet). Elemental analyses were performed by Atlantic Microlab Inc. For each procedure, "standard workup" refers to the following steps: addition of indicated organic solvent, washing the organic layer with water then brine, separation of the organic layer from the aqueous layer, drying the combined organic layers with anhydrous sodium sulfate, filtering off the sodium sulfate, and removing the organic solvent under reduced pressure.

4-Amino-4′-hydroxystilbene (2a). Stannous chloride (11.8 g, 0.062 mol) was added to a solution of compound **1a** (Frinton Lab) (3.0 g, 0.012 mol) in ethanol (100 mL) followed by the addition of concentrated hydrochloric acid (5.0 mL). The solution was brought to reflux for 3 h and cooled to room temperature stirring overnight. Aqueous sodium hydroxide (1 N) was added to adjust the pH to 8−9. After standard workup with dichloromethane, crude product **2a** was obtained and was used in the following step without further purifications. **2a** (2.6 g, ∼100%): ^{1}H NMR (DMSO-d_6) δ 9.39 (s, 1H), 7.30 (d, 2H, J = 8.5 Hz), 7.20 (d, 2H, J = 8.5 Hz), 6.80 (m, 2H), 6.72 (d, 2H, J = 8.5 Hz), 6.53 (d, 2H, J = 8.5 Hz), 5.19 (s, 2H).

4-*N*,*N*′-Dimethylamino-4′-hydroxystilbene (3a). To a mixture of **2a** (211 mg, 1.0 mmol), paraformaldehyde (300 mg, 10 mmol), and sodium cyanoborohydride (189 mg, 3.0 mmol) was added acetic acid (10 mL). The whole mixture was stirred at room-temperature overnight and then poured into 100 mL of water. Sodium carbonate was added to adjust the pH to 8−9. After standard workup with 5% methanol in dichloromethane, the residue was purified by silica gel column chromatography (2.5% methanol in dichloromethane) to afford **3a** as a white solid (214 mg, 89.5%): ^{1}H NMR δ 7.37 (m, 4H), 6.87 (s, 2H), 6.75 (m, 4H), 4.68 (s, 1H), 2.98 (s, 6H).

(4-{2-[4-(2,2-Dimethyl-[1,3]dioxan-5-ylmethoxy)phenyl]-vinyl}phenyl)dimethylamine (3b). Under a nitrogen atmosphere, **3a** (100 mg, 0.38 mmol) was dissolved in anhydrous DMF (5.0 mL). Potassium carbonate (140 mg, 1.0 mmol) was added to this solution followed by 5-bromomethyl-2,2-dimethyl-[1,3]dioxane **8m**[24] (105 mg, 0.5 mmol). The mixture was heated to 100 °C and stirred overnight. After cooling to room temperature, standard workup with dichloromethane was applied and the residue was purified by silica gel preparative TLC (1% methanol in dichloromethane) to afford compound **3b** (100 mg, 72%): ^{1}H NMR δ 7.38 (m, 4H), 6.88 (m, 4H), 6.70 (d, 2H, J = 8.7 Hz), 4.08 (m, 4H), 3.87 (m, 2H), 2.96 (s, 6H), 2.13 (m, 1H), 1.46 (s, 3H), 1.42 (s, 3H). Anal. ($C_{23}H_{29}NO_3$) C, H, N.

2-{4-[2-(4-Dimethylaminophenyl)vinyl]phenoxymethyl}-propane-1,3-diol (3c). Compound **3b** (180 mg, 0.49 mmol) was suspended in acetone (5.0 mL) and cooled to 0 °C with an ice bath. 1 N HCl (5.0 mL, 5.0 mmol) was slowly added over 20 min. The suspension turned into a clear solution during the addition. The solution was stirred at 0 °C for an additional 1.5 h and then warmed to room temperature in 0.5 h. Saturated sodium bicarbonate was added to adjust pH to 8−9. After standard workup with dichloromethane, the residue was purified by silica gel preparative TLC (5% methanol in dichloromethane) to afford compound **3c** as a white solid (140 mg, 87%): ^{1}H NMR δ 7.40 (m, 4H), 6.88 (m, 4H), 6.74 (m, 2H), 4.10 (d, 2H, J = 5.47 Hz), 3.89 (d, 4H, J = 5.28 Hz), 2.98 (s, 6H), 2.22 (m, 1H). Anal. ($C_{20}H_{25}NO_3$) C. H. N.

Toluene-4-sulfonic Acid 3-{4-[2-(4-(Dimethylamino)phenyl)vinyl]phenoxy}-2-hydroxymethylpropyl Ester (3d). Compound **3c** (158 mg, 0.49 mmol) was dissolved in anhydrous pyridine (15 mL) and cooled to 0 °C with an ice bath. Tosyl chloride (137 mg, 0.72 mmol) was added, and the solution was stirred at 0 °C for 2 h. After standard workup with dichloromethane, the residue was purified by silica gel preparative TLC (5% methanol in dichloromethane) to afford monotosylate compound **3d** as a white solid (95 mg, 41%): ^{1}H NMR δ 7.75 (d, 2H, J = 8.26 Hz), 7.37 (m, 4H), 7.26 (m, 2H), 6.88 (m, 2H), 6.72 (m, 4H), 4.26 (d, 2H, J = 5.66 Hz), 3.97 (d, 2H, J = 5.96 Hz), 3.79 (d, 2H, J = 5.24 Hz), 2.95 (s, 6H), 2.38 (m, 4H). Anal. ($C_{27}H_{31}NO_5S$) C, H, N.

3-{4-[2-(4-Dimethylaminophenyl)vinyl]phenoxy}-2-fluoromethylpropan-1-ol (3e). Compound **3d** (40 mg, 0.083 mmol) was dissolved in anhydrous THF (5.0 mL). Under a nitrogen atmosphere, anhydrous TBAF [25] (150 mg, 0.5 mmol) in anhydrous THF (1.0 mL) was slowly added. The solution was then heated to reflux for 3 h. After cooling to room temperature, standard workup with dichloromethane was applied and the residue was applied for silica gel preparative TLC (5% methanol in dichloromethane) to afford product **3e** (17 mg, 62%): ^{1}H NMR δ 7.40 (m, 4H), 6.89 (m, 4H), 6.70 (d, 2H, J = 8.82 Hz), 4.67 (d d, 2H, J_1 = 47.1 Hz, J_2 = 5.46 Hz), 4.10 (d, 2H, J = 5.86 Hz), 3.88 (d, 2H, J = 5.24 Hz), 2.97 (s, 6H), 2.40 (m, 1H), 1.76 (s, 1H). Anal. ($C_{20}H_{24}FNO_2$) C, H, N.

2,2-Dimethyl-5-{4-[2-(4-nitrophenyl)vinyl]phenoxymethyl}-[1,3]dioxane (1b). Compound **1b** was prepared from **1a** (241 mg, 1.0 mmol) with the same procedure described for compound **3b**. **1b** (260 mg, 70%): ^{1}H NMR δ 8.19 (d, 2H, J = 8.80 Hz), 7.49 (m, 4H), 7.07 (m, 2H), 6.90 (d, 2H, J = 8.80 Hz), 4.12 (m, 4H), 3.89 (d, 2H), 2.10 (m, 1H), 1.48 (s, 3H), 1.43 (s, 3H). Anal. Calcd. ($C_{21}H_{23}NO_5$) C, H, N.

2-{4-[2-(4-Nitrophenyl)vinyl]phenoxymethyl}propane-1,3-diol (1c). Compound **1c** was prepared from **1b** (260 mg, 0.7 mmol) with the same procedure described for compound **3c**. **1c** (190 mg, 82%): ^{1}H NMR (CD_3OD) δ 8.19 (d, 2H, J = 8.80 Hz), 7.72 (d, 2H, J = 8.80 Hz), 7.55 (d, 2H, J = 8.70 Hz), 7.24 (q, 2H), 6.96 (d, 2H, J = 8.70 Hz), 4.09 (d, 2H, J = 5.78 Hz), 3.74 (d, 4H, J = 5.94 Hz), 2.14 (m, 1H). Anal. ($C_{18}H_{19}NO_5$) C, H, N.

Toluene-4-sulfonic Acid 2-Hydroxymethyl-3-{4-[2-(4-nitrophenyl)vinyl]phenoxy}propyl Ester (1d). Compound **1d** was prepared from **1c** (80 mg, 0.24 mmol) with the same procedure described for compound **3d**. **1d** (66 mg, 56%): ^{1}H NMR δ 8.18 (d, 2H, J = 8.82 Hz), 7.77 (d, 2H, J = 8.32 Hz), 7.58 (d, 2H, J = 8.82 Hz), 7.45 (d, 2H, J = 8.73 Hz), 7.28 (d, 2H, J = 8.18 Hz), 7.09 (q, 2H), 6.81 (d, 2H, J = 8.73 Hz), 4.27 (d, 2H, J = 5.70 Hz), 4.01 (m, 2H), 3.80 (d, 2H, J = 5.61 Hz), 2.40 (m, 4H), 2.02 (s, 1H). Anal. ($C_{25}H_{25}NO_7S$) C, H, N.

2-Fluoromethyl-3-{4-[2-(4-nitrophenyl)vinyl]phenoxy}-propan-1-ol (1e). Compound **1e** was prepared from **1d** (33 mg, 0.069 mmol) with the same procedure described for compound **3e**. **1e** (20 mg, 88%): ^{1}H NMR δ 8.19 (d, 2H, J = 8.83 Hz), 7.58 (d, 2H, J = 8.84 Hz), 7.48 (d, 2H, J = 8.74 Hz), 7.10 (q, 2H), 6.94 (d, 2H, J = 8.68 Hz), 4.69 (d d, 2H, J_1 = 47.1 Hz, J_2 = 5.36 Hz), 4.15 (d, 2H, J = 5.89 Hz), 3.90 (d, 2H, J = 5.43 Hz), 2.43 (m, 1H), 1.74 (s, 1H). Anal. ($C_{18}H_{18}FNO_4$) C, H, N.

3-{4-[2-(4-Aminophenyl)vinyl]phenoxy}-2-fluoromethylpropan-1-ol (2e). Compound **2e** was prepared from **1e** (37 mg, 0.11 mmol) with the same procedure described for compound **2a**. **2e** (24 mg, 71%): ^{1}H NMR δ 7.35 (m, 4H), 6.90 (m, 4H), 6.66 (d, 2H, J = 8.54 Hz), 4.69 (d d, 2H, J_1 = 47.1 Hz, J_2 = 5.46 Hz), 4.12 (d, 2H, J = 5.84 Hz), 3.90 (d, 2H, J = 5.56 Hz), 3.70 (s, 2H), 2.39 (m, 1H), 1.71 (s, 1H). Anal. ($C_{18}H_{20}FNO_2$) C, H, N.

2-Fluoromethyl-3-{4-[2-(4-methylaminophenyl)vinyl]-phenoxy}propan-1-ol (4e). Under a nitrogen atmosphere, sodium methoxide (22 mg, 0.4 mmol) was added to a suspension of compound **2e** (24 mg, 0.08 mmol) in methanol (6 mL) followed by paraformaldehyde (12 mg, 0.4 mmol). The solution was heated to reflux for 2 h and cooled to 0 °C with an ice bath. Sodium borohydride (15 mg, 0.4 mmol) was added in portions. Reaction mixture was brought to reflux again for 1 h and poured onto crushed ice. After standard workup with dichloromethane, the residue was applied for silica gel preparative TLC (4.5% methanol in dichloromethane) to afford product **4e** (23 mg, 92%): ^{1}H NMR δ 7.37 (m, 4H), 6.87 (m, 4H), 6.59 (d, 2H, J = 8.56 Hz), 4.69 (d, d, 2H, J_1 = 47.1 Hz, J_2 = 5.44 Hz), 4.12 (d, 2H, J = 5.86 Hz), 4.00 (s, 1H), 3.89. (d, 2H, J = 5.52 Hz), 2.86 (s, 3H), 2.41 (m, 1H), 1.75 (s, 1H). Anal. ($C_{19}H_{22}FNO_2$) C, H, N.

4-*N*-Methylamino-4′-hydroxystilbene (4a). Compound **4a** was prepared from **2a** (105 mg, 0.5 mmol) with the same procedure as described for compound **4e**. **4a** (100 mg, 89%): ^{1}H NMR δ 7.34 (m, 4H), 6.86 (s, 2H), 6.79 (d, 2H, J = 8.58 Hz), 6.60 (d, 2H, J = 8.58 Hz), 2.85 (s, 3H).

(2,2-Di-*tert*-butyl-[1,3,2]dioxasilinan-5-yl)-methanol (7n). To the solution of 2-hydroxypropyl-1,3-diol **6** (500 mg, 4.7 mmol) in anhydrous dichloromethane (15 mL) was added HOBT(135 mg, 1.0 mmol). Under a nitrogen atmosphere, triethylamine (6.5 mL, 4.9 g, 48 mmol) was added via a syringe followed by di-*tert*-butyldichlorosilane (1.05 g, 5.0 mmol). The solution was gently refluxed for 1 h and cooled to room temperature. After standard workup with dichloromethane, the residue was applied for silica gel column chromatography (1% methanol in dichloromethane) to afford product **7n**, which was used for the following step without further purification. **7n** (1.03 g, 89%): ^{1}H NMR δ 4.17 (m, 2H), 3.92 (t, 2H), 3.50 (d, 2H, J = 5.78 Hz), 2.30 (m, 1H), 1.39 (s, 1H), 1.04 (s, 9H), 1.02 (s, 9H).

5-Bromomethyl-2,2-di-*tert*-butyl-[1,3,2]dioxasilinane (8n). Compound **7n** (123 mg, 0.5 mmol) was dissolved in dichloromethane (10 mL) and cooled to −10 °C with an ethanol-ice bath. Pyridine (1 mL) was added followed by carbon tetrabromide (220 mg, 0.66 mmol). Triphenylphosphine (174 mg, 0.66 mmol) was added in portions, and the solution was stirred at −10 °C for 2 h then raised to room-temperature overnight. Solvent was removed under reduced pressure, and residue was applied for silica gel column chromatography (10% ethyl acetate in hexane) to afford compound **8n**, which was used in the following step without further purification. **8n** (130 mg, 84%): ^{1}H NMR δ 4.20 (m, 2H), 3.93 (t, 2H), 3.20 (d, 2H, J = 6.19 Hz), 2.39 (m, 1H), 1.04 (s, 9H), 1.01 (s, 9H).

(4-{2-[4-(2,2-Di-*tert*-butyl-[1,3,2]dioxasilinan-5-ylmethoxy)phenyl]vinyl}phenyl)methylamine (4f). Under a nitrogen atmosphere, compound **4a** (90 mg, 0.4 mmol) was dissolved in anhydrous DMF (15.0 mL). Potassium carbonate (560 mg, 4.0 mmol) was added followed by 5-bromomethyl-2,2-di-*tert*-butyl-[1,3,2]dioxasilinane, **8n** (127 mg, 0.4 mmol). The suspension was heated to 100 °C and stirred overnight. After cooling to room temperature, standard workup with dichloromethane was applied and the residue was purified by silica gel preparative TLC (dichloromethane) to afford compound **4f** (115 mg, 63%): ^{1}H NMR δ 7.38 (m, 4H), 6.88 (s, 2H), 6.82 (d, 2H, J = 8.64 Hz), 6.73 (d, 2H, J = 8.42), 5.80 (s, 1H), 4.26 (m, 2H), 4.04 (t, 2H), 3.81 (d, 2H, J = 5.82 Hz), 2.89 (s, 3H), 2.58 (m, 1H), 1.06 (s, 9H), 1.04 (s, 9H). Anal. ($C_{27}H_{39}NO_3Si$) C, H, N.

(4-{2-[4-(2,2-Di-*tert*-butyl-[1,3,2]dioxasilinan-5-ylmethoxy)phenyl]vinyl}phenyl)methylcarbamic Acid *tert*-Butyl Ester (5f). BOC anhydride (320 mg, 1.46 mmol) was added to a solution of compound **4f** (110 mg, 0.24 mmol) in anhydrous THF (10 mL). Under the protection of nitrogen, triethylamine (1.0 mL) was added via a syringe. The solution was then refluxed for 34 h. After cooling to room temperature, standard workup with dichloromethane was applied. Organic solvent was removed under reduced pressure, and the residue was purified through silica gel column chromatography to afford compound **5f**, which was used in the following step without further purification. **5f** (122 mg, 91%): ^{1}H NMR δ 7.42 (d, 4H, J = 7.52 Hz), 7.20 (d, 2H, J = 8.52 Hz), 6.98 (m, 2H), 6.84 (d, 2H, J = 8.72 Hz), 4.26 (m, 2H), 4.05 (t, 2H), 3.82 (d, 2H, J = 5.84 Hz), 3.27 (s, 3H), 2.58 (m, 1H), 1.46 (s, 9H), 1.06 (s, 9H), 1.04 (s, 9H).

(4-{2-[4-(3-Hydroxy-2-hydroxymethylpropoxy)phenyl]-vinyl}phenyl)methylcarbamic Acid *tert*-Butyl Ester (5c). Compound **5f** (120 mg, 0.22 mmol) was dissolved in anhydrous THF (10 mL), and the solution was cooled to 0 °C with an ice bath. Under a nitrogen atmosphere, TBAF (0.44 mL, 1 M in THF, 0.44 mmol) was added via a syringe. The solution was stirred at 0 °C for 0.5 h and then brought to room temperature for another 2 h. After standard workup with dichloromethane, the residue was applied for silica gel preparative TLC (5% methanol in dichloromethane) to afford compound **5c** (89 mg, 99%): ^{1}H NMR δ 7.43 (d, 4H, J = 8.68 Hz), 7.20 (d, 2H, J = 8.56 Hz), 6.98 (m, 2H), 6.90 (d, 2H, J = 8.74 Hz), 4.14 (d, 2H, J = 5.96 Hz), 3.95 (d, 4H, J = 5.24 Hz), 3.27 (s, 3H), 2.27 (m, 1H), 1.70 (s, 2H), 1.46 (s, 9H). Anal. ($C_{24}H_{31}NO_5$) C, H, N.

[4-(2-{4-[2-Hydroxymethyl-3-(tetrahydropyran-2-yloxy)-propoxy]phenyl}vinyl)phenyl]methylcarbamic Acid *tert*-butyl Ester (5g). A solution of **5c** (53 mg, 0.13 mmol) and 3, 4-dihydropyran (12.9 mg, 0.15 mmol) in dry dichloromethane (12 mL) containing pyridinium *p*-toluenesulfonate[26] (3.3 mg, 0.013 mol) was stirred at room temperature for 4 h. After standard workup with dichloromethane, the residue was applied for silica gel preparative TLC (5% methanol in dichloromethane) to afford compound **5g**, which was used in the following step without further purifications. **5g** (43 mg, 67%): ^{1}H NMR δ 7.43 (d, 4H, J = 8.46 Hz), 7.20 (d, 2H, J = 8.46 Hz), 6.97 (m, 2H), 6.90 (d, 2H, J = 8.62 Hz), 4.60(b, 1H), 3.95 (m, 6H), 3.70 (m, 1H), 3.54 (m, 1H), 3.26 (s, 3H), 2.34 (m, 1H), 1.70 (m, 6H), 1.46 (s, 9h).

Methanesulfonic Acid 3-(4-{2-[4-(*tert*-Butoxycarbonylmethylamino)phenyl]vinyl}phenoxy)-2-(tetrahydropyran-2-yloxymethyl)propyl Ester (5h). Triethylamine (0.2 mL) was added to a solution of compound **5g** (43 mg, 0.087 mmol) and methanesulfonyl chloride (29.7 mg, 0.26 mmol) in dry dichloromethane (10 mL). The solution was stirred at room temperature for 3.5 h. After standard workup with dichloromethane, the residue was applied for silica gel preparative TLC (2% methanol in dichloromethane) to afford compound **5h** (43 mg, 86%): ^{1}H NMR δ 7.43 (d, 4H, J = 8.58 Hz), 7.20 (d, 2H, J = 8.46 Hz), 6.97 (m, 2H), 6.90 (d, 2H, J = 8.62 Hz), 4.59(b, 1H), 4.46 (d, 2H, J = 5.66 Hz), 4.11 (m, 2H), 3.85 (m, 2H), 3.55 (m, 2H), 3.27 (s, 3H), 3.00 (s, 3H), 2.59 (m, 1H), 1.70 (m, 6H), 1.46 (s, 9h). HRMS m/Z calcd. For $C_{30}H_{41}NO_8S$ (M^+-Na^+): 598.2451. Found: 598.2444.

2-{4-[2-(4-Aminophenyl)vinyl]phenoxymethyl}propane-1,3-diol (2c). Compound **2c** was prepared from **1b** (200 mg, 0.54 mmol) with the same procedure described for **2a** and was used in the following step without further purifications. **2c** (144 mg, 89%): ^{1}H NMR (DMSO-d_6) δ 7.40 (d, 2H, J = 8.58 Hz), 7.22 (d, 2H, J = 8.30 Hz), 6.91 (m, 4H), 6.54 (d, 2H, J = 8.30 Hz), 5.22 (s, 2H), 4.51 (t, 2H, J = 5.11 Hz), 3.97 (d, 2H, J = 5.85 Hz), 3.51 (t, 4H), 1.96 (m, 1H).

2-{4-[2-(4-Methylaminophenyl)vinyl]phenoxymethyl}propane-1,3-diol (4c). Compound **4c** was prepared from **2c** (100 mg, 0.33 mmol) with the same procedure described for **4a**. **4c** (104 mg, 99%): ^{1}H NMR (DMSO-d_6) δ 7.42 (d, 2H, J = 8.58 Hz), 7.30 (d, 2H, J = 8.46 Hz), 6.88 (m, 4H), 6.52 (d, 2H, J = 8.42 Hz), 5.80 (m, 1H), 4.51 (t, 2H), 3.97 (d, 2H, J = 5.85 Hz), 3.51 (t, 4H, J = 5.95 Hz), 2.68 (d, 3H, J = 4.7 Hz), 1.95 (m, 1H). Anal. ($C_{19}H_{23}NO_3$) C, H, N.

2-(4-Bromobenzyl)propane-1,3-diol (10). 2-(4-Bromobenzyl)malonic acid diethyl ester **9** [27] (1.5 g, 3.8 mmol) was dissolved in 5 mL of THF, and the solution was added slowly to DIBALH (1 M in toluene, 25 mL) via a syringe at 0 °C and stirred at the same temperature for 3 h. HCl (2 N, 50 mL) was then added to break the complex. After standard workup with ethyl acetate, crude product **10** (0.9 g, 99%) was obtained, which was used directly for the next step without further purification: ^{1}H NMR δ 7.39 (d, 2H, J = 8.2 Hz), 7.04 (d, 2H, J = 8.2 Hz), 3.60 (m, 4H), 2.55 (d, 2H, J = 7.4 Hz), 1.96 (m, 1H).

3-(4-Bromophenyl)-2-(*tert*-butyldimethylsilanyloxymethyl)propan-1-ol (11). Under a nitrogen atmosphere, *tert*-butyl-chloro-dimethylsilane (246 mg, 1.63 mmol) was added to a solution of compound **10** (400 mg, 1.63 mmol) in dichloromethane (10 mL) at 0 °C, followed by triethylamine (412 mg, 4.07 mmol). The solution was gradually warmed to room temperature and stirred overnight. After standard work up with dichloromethane, the residue was purified by silica gel preparative TLC (40% ethyl acetate in hexane) to afford compound **11** (370 mg, 63.2%): ^{1}H NMR δ 7.41 (d, 2H, J = 6.6 Hz), 7.08 (d, 2H, J = 6.6 Hz), 3.66 (m, 4 H), 2.60 (m, 2H), 1.94 (m, 1H), 0.91 (s, 9H), 0.06 (s, 6H).

[2-Bromomethyl-3-(4-bromophenyl)propoxy]-*tert*-butyldimethylsilane (12). Compound **12** was prepared from **11** (80 mg, 0.22 mmol) with the same procedure described for **8m** [24] and was used in the following step without further purifications. **12** (70 mg, 75%): ^{1}H NMR δ 7.40 (d, 2H, J = 6.6 Hz), 7.07 (d, 2H, J = 6.6 Hz), 3.46 (m, 4H), 2.73 (d, 2H, J = 7.2 Hz), 2.03 (m, 1H), 0.94 (s, 9H), 0.06 (s, 6H).

[4-(2-{4-[2-(4-Bromobenzyl)-3-(*tert*-butyldimethylsilanyloxy)propoxy]phenyl}vinyl)phenyl]dimethylamine (3i). Compound **3i** was prepared from **12** (50 mg, 0.12 mmol) and **3a** (28 mg, 0.12 mmol) with the same procedure for **3b**. This product was used in the following step without further purifications. **3i** (40 mg, 59%). ^{1}H NMR δ 7.40 (m, 6H), 7.09 (d, 2H, J = 8.2 Hz), 6.84 (m, 4H), 6.72 (d, 2H, J = 8.8 Hz), 3.91 (d, 2H, J = 5.4 Hz), 3.67 (m, 2H), 2.99 (s, 6H), 2.75 (d, 2H, J = 7.4 Hz), 2.20 (m, 1H), 0.91 (s, 9H), 0.04 (s, 6H).

2-(4-Bromobenzyl)-3-{4-[2-(4-(dimethylamino)phenyl)vinyl]phenoxy}propan-1-ol (3j). Compound **3j** was prepared from **3i** (40 mg, 0.069 mmol) with the same procedure described for **5c**. **3j** (19 mg, 59%): ^{1}H NMR δ: 7.40 (m, 4H), 7.07 (d, 2H, J = 8.2 Hz), 6.87 (m, 4H), 6.70 (d, 2H, J = 8.2 Hz), 3.94(m, 2H), 3.75 (b, 2H), 2.97 (s, 6H), 2.76 (d, 2H, J = 7.4 Hz), 2.23 (m, 1H), 1.78 (s, 1H). Anal. ($C_{26}H_{28}BrNO_2$) C, H, N.

[^{18}F]3-{4-[2-(4-Dimethylaminophenyl)vinyl]phenoxy}-2-fluoromethylpropan-1-ol ([^{18}F]3e). [^{18}F]Fluoride, produced by a cyclotron using ^{18}O(p,n)^{18}F reaction, was passed through a Sep-Pak Light QMA cartridge as an aqueous solution in [^{18}O]-enriched water. The cartridge was dried by airflow, and the ^{18}F activity was eluted with 2 mL of Kryptofix 222 (K222)/K_2CO_3 solution (22 mg of K222 and 4.6 mg of K_2CO_3 in CH_3CN/H_2O 1.77/0.23). The solvent was removed at 120 °C under an argon stream. The residue was azeotropically dried with 1 mL of anhydrous CH_3CN twice at 120 °C under an argon stream. A solution of tosylate precursor **3d** (4 mg) in DMSO (0.2 mL) was added to the reaction vessel containing the dried ^{18}F activities. The solution was heated at 120 °C for 4 min. Water (2 mL) was added, and the mixture was extracted with ethyl acetate (1 mL × 2). The combined organic layer was dried (Na_2SO_4), and the solvent was removed using an argon stream with gentle heating (55−60 °C). The residue was dissolved in CH_3CN and injected to HPLC for purification [Hamilton PRP-1 column (7.0 × 305 mm, 10 μm); CH_3CN/dimethyl glutarate buffer (5 mM, pH 7) = 9/1; flow rate = 2 mL/min). Retention time of **3e** was 11 min and well separated from precursor **3d** (t_R = 13 min). The same HPLC condition was used for quality control (RCP > 99%). Specific activity was estimated by comparing UV peak intensity of purified **[^{18}F]3e** with a reference nonradioactive compound of known concentration. Specific activity was estimated to be 70 Ci/mmol after the preparation.

[^{18}F]2-Fluoromethyl-3-{4-[2-(4-methylaminophenyl)-vinyl]phenoxy}propan-1-ol ([^{18}F]4e). The labeling reaction was carried out as described above for dimethylamino compound. The mesylate **5h** (4 mg) was used as the precursor for the labeling. After the initial reaction at 120°C in DMSO, 1 mL of H_2O was added and the solution was cooled for 1 min. 1 mL of 10% HCl was then added, and the mixture was heated at 120°C again for 10 min. Aqueous solution of NaOH was added to adjust the pH to basic. The mixture was extracted with ethyl acetate (1 mL × 2), the combined organic layer was dried (Na_2SO_4), and the solvent was removed under argon stream with gentle heating (55−60 °C). The residue was dissolved in CH_3CN and injected to HPLC for purification [Hamilton PRP-1 column (7.0 × 305 mm, 10 μm); CH_3CN/dimethyl glutarate buffer (5 mM, pH 7) = 9/1; flow rate = 2 mL/min). Retention time of **4e** was 10 min and well separated from precursor **5h** (t_R = 13 min) as well as the hydrolysis byproduct of precursor (t_R = 8 min). The same HPLC condition was used for quality control (RCP > 99%). Specific activity was estimated by comparing UV peak intensity of purified **[^{18}F]4e** with reference nonradioactive compound of known concentration. Specific activity was estimated to be 900−1000 Ci/mmol after the preparation.

Preparation of Brain Tissue Homogenates. Postmortem brain tissues were obtained from control and AD patients at autopsy, and neuropathological diagnosis was confirmed by current criteria (NIA-Reagan Institute Consensus Group, 1997). Homogenates were then prepared from dissected gray and white matters from pooled control and AD patients in phosphate buffered saline (PBS, pH 7.4) at the concentration of approximately 100 mg wet tissue/mL (motor-driven glass homogenizer with setting of 6 for 30 s). The homogenates were aliquoted into 1-mL portions and stored at −70 °C for 3−6 months without loss of binding signal.

Binding Studies. [^{125}I]IMPY with 2200 Ci/mmol specific activity and greater than 95% radiochemical purity was prepared using the standard iododestannylation reaction and purified by a simplified C-4 minicolumn as described previously.[18] Binding assays were carried out in 12 × 75 mm borosilicate glass tubes. The reaction mixture contained 50 μL of brain homogenates (20−50 μg), 50 μL of [^{125}I]IMPY (0.04−0.06 nM diluted in PBS) and 50 μL of inhibitors (10^{-5}−10^{-10} M diluted serially in PBS containing 0.1% bovine serum

albumin, BSA) in a final volume of 1 mL. Nonspecific binding was defined in the presence of IMPY (600 nM) in the same assay tubes. A similar assay condition for [^{18}F]**4e** was used for binding in a range of concentration between 0.3 and 0.5 nM. The nonspecific binding was defined in the presence of nonradioactive **4e** (1000 nM). The mixture was incubated at 37°C for 2 h, and the bound and the free radioactivity were separated by vacuum filtration through Whatman GF/B filters using a Brandel M-24R cell harvester followed by 2 × 3 mL washes of PBS at room temperature. Filters containing the bound ^{125}I or ^{18}F ligand were assayed for radioactivity content in a gamma counter (Packard 5000) with 70% counting efficiency. Under the assay conditions, the specifically bound fraction was less than 15% of the total radioactivity. The results of inhibition experiments were subjected to nonlinear regression analysis using EBDA by which K_i values were calculated.

Film Autoradiography. Brain sections from AD subjects were obtained by freezing the brain in powdered dry ice and cut into 20-μm thick sections. The sections were incubated with [^{18}F]tracers (200 000−250 000 cpm/200 μL) for 1 h at room temperature. The sections were then dipped in saturated Li_2CO_3 in 40% EtOH (two 2 min washes) and washed with 40% EtOH (one 2 min wash) followed by rinsing with water for 30 s. After drying, the ^{18}F-labeled sections were exposed to Kodak MR film overnight.

In Vivo Plaque Labeling with [^{18}F]3e and [^{18}F]4e. The in vivo evaluation was performed using either double transgenic APP/PS1 or single transgenic APP2576 mice which were kindly provided by AstraZeneca. After anesthetizing with 1% isoflurane, 250−300 μCi of [^{18}F]**3e** or [^{18}F]**4e** in 200 μL of 0.1% BSA solution was injected through the tail vein. The animals were allowed to recover for 60−120 min and then killed by decapitation. The brains were immediately removed and frozen in powdered dry ice. Sections of 20 μm were cut and exposed to Kodak MR film for overnight. Ex vivo film autoradiograms were thus obtained.

Organ Distribution in Normal Mice. While under isoflurane anesthesia, 0.15 mL of a 0.1% bovine serum albumin solution containing [^{18}F]tracers (5−10 μCi) were injected directly into the tail vein of ICR mice (22−25 g, male) The mice (n = 3 for each time point) were sacrificed by cervical dislocation at 120 min postinjection. The organs of interest were removed and weighed, and the radioactivity was assayed for radioactivity content with an automatic gamma counter. The percentage dose per organ was calculated by a comparison of the tissue counts to suitably diluted aliquots of the injected material. Total activities of blood were calculated under the assumption that they were 7% of the total body weight. The % dose/g of samples was calculated by comparing the sample counts with the count of the diluted initial dose.

Partition Coefficient. Partition coefficients were measured by mixing the [^{18}F]tracer with 3 g each of 1-octanol and buffer (0.1 M phosphate, pH 7.4) in a test tube. The test tube was vortexed for 3 min at room temperature, followed by centrifugation for 5 min. Two weighed samples (0.5 g each) from the 1-octanol and buffer layers were counted in a well counter. The partition coefficient was determined by calculating the ratio of cpm/g of 1-octanol to that of buffer. Samples from the 1-octanol layer were re-partitioned until consistent partitions of coefficient values were obtained (usually the 3rd or 4th partition). The measurement was done in triplicate and repeated three times.

Acknowledgment. This work was supported by the grant from the National Institute of Health (AG022559 to H.F.K). APP/PS1 and Tg2576 transgenic mice were kindly provided by AstraZeneca. PIB was kindly provided by Dr. A Verbruggen in Katholieke Universiteit, Leuven.

Supporting Information Available: Elemental analysis data are available for all prepared compounds. This material is available free of charge via the Internet at http://pubs.acs.org.

References

(1) Hardy, J.; Selkoe, D. J. The amyloid hypothesis of Alzheimer's disease: progress and problems on the road to therapeutics. *Science* **2002**, *297*, 353−356.
(2) Ginsberg, S. D.; Schmidt, M. L.; Crino, P. B.; Eberwine, J. H.; Lee, V. M.-Y.; Trojanowski, J. Q. Molecular pathology of Alzheimer's disease and related disorders. *Cerebral cortex: neurodegenerative and age-related changes in structure and function of cerebral cortex*; Kluwer Academic/Plenum: New York, 1999; pp 603−654.
(3) Selkoe, D. J. Imaging Alzheimer's amyloid. *Nature Biotechnol.* **2000**, *18*, 823−824.
(4) Wolfe, M. S. Therapeutic strategies for Alzheimer's disease. *Nat. Rev. Drug Discovery* **2002**, *1*, 859−866.
(5) Bachurin, S. O. Medicinal chemistry approaches for the treatment and prevention of Alzheimer's disease. *Med. Res. Rev.* **2003**, *23*, 48−88.
(6) Klunk, W. E.; Engler, H.; Nordberg, A.; Wang, Y.; Blomqvist, G.; Holt, D. P.; Bergstrom, M.; Savitcheva, I.; Huang, G.-f.; Estrada, S.; Ausen, B.; Debnath, M. L.; Barletta, J.; Price, J. C.; Sandell, J.; Lopresti, B. J.; Wall, A.; Koivisto, P.; Antoni, G.; Mathis, C. A.; Langstrom, B. Imaging Brain Amyloid in Alzheimer's Disease with Pittsburgh Compound-B. *Ann. Neurol.* **2004**, *55*, 306−319.
(7) Verhoeff, N. P.; Wilson, A. A.; Takeshita, S.; Trop, L.; Hussey, D.; Singh, K.; Kung, H. F.; Kung, M.-P.; Houle, S. In vivo imaging of Alzheimer disease beta-amyloid with [11C]SB-13 PET. *Am. J. Geriatr. Psychiatry* **2004**, *12*, 584−595.
(8) Okamura, N.; Suemoto, T.; Shimadzu, H.; Suzuki, M.; Shiomitsu, T.; Akatsu, H.; Yamamoto, T.; Staufenbiel, M.; Yanai, K.; Arai, H.; Sasaki, H.; Kudo, Y.; Sawada, T. Styrylbenzoxazole derivatives for in vivo imaging of amyloid plaques in the brain. *J. Neurosci.* **2004**, *24*, 2535−2541.
(9) Shoghi-Jadid, K.; Small, G. W.; Agdeppa, E. D.; Kepe, V.; Ercoli, L. M.; Siddarth, P.; Read, S.; Satyamurthy, N.; Petric, A.; Huang, S. C.; Barrio, J. R.; Liu, J.; Flores-Torres, S.; Cole, G. M. Localization of neurofibrillary tangles and beta-amyloid plaques in the brains of living patients with Alzheimer disease: Binding characteristics of radiofluorinated 6-dialkylamino-2-naphthylethylidene derivatives as positron emission tomography imaging probes for beta-amyloid plaques in Alzheimer disease. *Am. J. Geriatr. Psychiatry* **2002**, *10*, 24−35.
(10) Mathis, C. A.; Wang, Y.; Klunk, W. E. Imaging b-amyloid plaques and neurofibrillary tangles in the aging human brain. *Curr. Pharm. Des.* **2004**, *10*, 1469−1492.
(11) Mathis, C. A.; Wang, Y.; Holt, D. P.; Huang, G.-f.; Debnath, M. L.; Klunk, W. E. Synthesis and Evaluation of ^{11}C-Labeled 6-Substituted 2-Arylbenzothiazoles as Amyloid Imaging Agents. *J. Med. Chem.* **2003**, *46*, 2740−2754.
(12) Wang, Y.; Klunk, W. E.; Debnath, M. L.; Huang, G. F.; Holt, D. P.; Shao, L.; Mathis, C. A. Development of a PET/SPECT agent for amyloid imaging in Alzheimer's disease. *J. Mol. Neurosci.* **2004**, *24*, 55−62.
(13) Agdeppa, E. D.; Kepe, V.; Liu, J.; Flores-Torres, S.; Satyamurthy, N.; Petric, A.; Cole, G. M.; Small, G. W.; Huang, S. C.; Barrio, J. R. Binding characteristics of radiofluorinated 6-dialkylamino-2-naphthylethylidene derivatives as positron emission tomography imaging probes for β-amyloid plaques in Alzheimer's disease. *J. Neurosci.* **2001**, *21*, RC189.
(14) Nordberg, A. PET imaging of amyloid in Alzheimer's disease. *Lancet Neurol.* **2004**, *3*, 519−527.
(15) Ono, M.; Wilson, A.; Nobrega, J.; Westaway, D.; Verhoeff, P.; Zhuang, Z.-P.; Kung, M.-P.; Kung, H. F. ^{11}C-Labeled Stilbene Derivatives as Aβ-aggregate-specific PET Imaging Agents for Alzheimer's Disease. *Nucl. Med. Biol.* **2003**, *30*, 565−571.
(16) Zhuang, Z. P.; Kung, M. P.; Wilson, A.; Lee, C. W.; Plossl, K.; Hou, C.; Holtzman, D. M.; Kung, H. F. Structure−activity relationship of imidazo[1,2-a]pyridines as ligands for detecting beta-amyloid plaques in the brain. *J. Med. Chem.* **2003**, *46*, 237−243.
(17) Kung, M. P.; Hou, C.; Zhuang, Z.-P.; Zhang, B.; Skovronsky, D. M.; Gur, T.; Lee, V. M.-Y.; Trojanowski, J. Q.; Kung, H. F. IMPY: An improved thioflavin-T derivative for in vivo Labeling of β-amyloid plaques. *Brain Res.* **2002**, *956*, 202−210.
(18) Kung, M.-P.; Hou, C.; Zhuang, Z.-P.; Cross, A. J.; Maier, D. L.; Kung, H. F. Characterization of IMPY as a potential imaging agent for β-amyloid plaques in double transgenic PSAPP mice. *Eur. J. Nucl. Med. Mol. Imag.* **2004**, *31*, 1136−1145.
(19) Kung, M.-P.; Hou, C.; Zhuang, Z.-P.; Skovronsky, D.; Kung, H. F. Binding of two potential imaging agents targeting amyloid plaques in postmortem brain tissues of patients with Alzheimer's disease. *Brain Res.* **2004**, *1025*, 89−105.

(20) Cai, L.; Chin, F. T.; Pike, V. W.; Toyama, H.; Liow, J.-S.; Zoghbi, S. S.; Modell, K.; Briard, E.; Shetty, U. H.; Sinclair, K.; Donohue, S.; Tipre, D.; Kung, M.-P.; Dagostin, C.; Widdowson, D. A.; Green, M.; Gao, W.; Herman, M. M.; Ichise, M.; Innis, R. B. Synthesis and Evaluation of Two ^{18}F-Labeled 6-Iodo-2-(4′-*N*,*N*-dimethylamino)phenylimidazo[1,2-*a*]pyridine Derivatives as Prospective Radioligands for *β*-Amyloid in Alzheimer's Disease. *J. Med. Chem.* **2004**, *47*, 2208−2218.

(21) Lee, C.-W.; Kung, M.-P.; Hou, C.; Kung, H. F. Dimethylaminofluorenes: Ligands for Detecting *β*-Amyloid Plaques in the Brain. *Nucl. Med. Biol.* **2003**, *30*, 573−580.

(22) Suemoto, T.; Okamura, N.; Shiomitsu, T.; Suzuki, M.; Shimadzu, H.; Akatsu, H.; Yamamoto, T.; Kudo, Y.; Sawada, T. In vivo labeling of amyloid with BF-108. *Neurosci. Res. (Amsterdam)* **2004**, *48*, 65−74.

(23) Kung, H. F.; Lee, C.-W.; Zhuang, Z. P.; Kung, M. P.; Hou, C.; Plossl, K. Novel stilbenes as probes for amyloid plaques. *J. Am. Chem. Soc.* **2001**, *123*, 12740−12741.

(24) Yuan, W.; Berman, R. J.; Gelb, M. H. Synthesis and evaluation of phospholipid analogues as inhibitors of cobra venom phospholipase A2. *J. Am. Chem. Soc.* **1987**, *109*, 8071−8081.

(25) Cox, D. P.; Terpinski, J.; Lawrynowicz, W. "Anhydrous" tetrabutylammonium fluoride: a mild but highly efficient source of nucleophilic fluoride ion. *J. Org. Chem.* **1984**, *49*, 3216−3219.

(26) Miyashita, N.; Yoshikoshi, A.; Grieco, A. P. Pyridinium *p*-toluenesulfonate. A mild and efficient catalyst for the tetrahydropyranylation of alcohols. *J. Org. Chem.* **1977**, *42*, 3772−3774.

(27) Musso, D. L.; Cochran, F. R.; Kelley, J. L.; McLean, E. W.; Selph, J. L. Indanylidenes.1. Design and Synthesis of (*E*)-2-(4,6-Difluoro-1-indanylidene)acetamide, a Potent, Centrally Acting Muscle Relaxant with Antiinflammatory and Analgesic Activity. *J. Med. Chem.* **2003**, *46*, 399−408.

(28) McGowan, E.; Sanders, S.; Iwatsubo, T.; Takeuchi, A.; Saido, T.; Zehr, C.; Yu, X.; Uljon, S.; Wang, R.; Mann, D.; Dickson, D.; Duff, K. Amyloid phenotype characterization of transgenic mice overexpressing both mutant amyloid precursor protein and mutant presenilin 1 transgenes. *Neurobiol. Dis.* **1999**, *6*, 231−244.

(29) Westerman, M. A.; Cooper-Blacketer, D.; Mariash, A.; Kotilinek, L.; Kawarabayashi, T.; Younkin, L. H.; Carlson, G. A.; Younkin, S. G.; Ashe, K. H. The relationship between Abeta and memory in the Tg2576 mouse model of Alzheimer's disease. *J. Neurosci.* **2002**, *22*, 1858−1867.

(30) van Dooren, T.; Dewachter, I.; Borghgraef, P.; van Leuven, F. Transgenic mouse models for APP processing and Alzheimer's disease: early and late defects. *Subcell Biochem.* **2005**, *38*, 45−63.

(31) Hsiao, K.; Chapman, P.; Nilsen, S.; Eckman, C.; Harigaya, Y.; Younkin, S.; Yang, F.; Cole, G. Correlative memory deficits, A*β* elevation, and amyloid plaques in transgenic mice. *Science* **1996**, *274*, 99−102.

(32) Cleary, J. P.; Walsh, D. M.; Hofmeister, J. J.; Shankar, G. M.; Kuskowski, M. A.; Selkoe, D. J.; Ashe, K. H. Natural oligomers of the amyloid-beta protein specifically disrupt cognitive function. *Nat. Neurosci.* **2005**, *8*, 79−84.

(33) Bitan, G.; Kirkitadze, M. D.; Lomakin, A.; Vollers, S. S.; Benedek, G. B.; Teplow, D. B. Amyloid beta -protein (Abeta) assembly: Abeta 40 and Abeta 42 oligomerize through distinct pathways. *Proc. Natl. Acad. Sci. U.S.A.* **2003**, *100*, 330−335.

(34) Serpell, L. C.; Sunde, M.; Benson, M. D.; Tennent, G. A.; Pepys, M. B.; Fraser, P. E. The protofilament substructure of amyloid fibrils. *J. Mol. Biol.* **2000**, *300*, 1033−1039.

JM050166G